Biocatalysis and Agricultural Biotechnology 17 (2019) 151–159

Contents lists available at ScienceDirect

Biocatalysis and Agricultural Biotechnology

journal homepage: www.elsevier.com/locate/bab

Investigation on characterization and biomedical properties of silver nanoparticles synthesized by an actinobacterium *Streptomyces olivaceus* (MSU3)

M. Sanjivkumar[a], R. Vaishnavi[a], M. Neelakannan[a], D. Kannan[a], T. Silambarasan[b], G. Immanuel[c,*]

[a] Department of Microbiology, K. R. College of Arts and Science, K.R. Nagar, Kovilpatti 628503, Tamilnadu, India
[b] Department of Microbiology, Periyar University, Salem 636011, Tamilnadu, India
[c] MNP Laboratory, Centre for Marine Science and Technology, Manonmaniam Sundaranar University, Rajakkamangalam 629502, Tamilnadu, India

ARTICLE INFO

Keywords:
Streptomyces sp
Bacterial pathogens
Silver nanoparticles
Antioxidant
XRD

ABSTRACT

This investigation was carried out to biosynthesize silver nanoparticles (AgNPs) from a marine actinobacterium *Streptomyces olivaceus* (MSU3), characterized its physical features and also evaluated its biomedical properties. Initially, AgNPs was produced by reduction of silver nitrate by using the selected actinobacterium under laboratory condition, followed by, the AgNPs was characterized using standard procedures. In FT-IR analysis, the biosynthesized AgNPs showed six major groups (C = C-H, ROH, C = N-OH, C-C, R-NH_2 and RCOOH) in between the wavenumber 455.20 and 3294.42 cm^{-1} and it expressed strong signal (3 keV) at silver region, which confirmed the formation of elemental silver by the reduction of silver ions with the absorption range of 450 nm. This biosynthesized AgNPs revealed spherical in shape and the particle size of 12.3 nm with the 2θ values of 38.12 – 77.41°. The antibacterial property of different concentrations of AgNPs was tested against clinical bacterial strains and it expressed maximum (23.0 mm) growth inhibition against *Streptococcus pneumoniae* at the highest concentration (30 µl) with the MIC and MBC values of 0.625 and ≤ 2.5 µg/ml respectively. Finally the *in-vitro* anti-inflammatory and antioxidant properties of AgNPs were assessed. It expressed the highest (97.53%) percentage inhibition of *in-vitro* anti-inflammatory activity at 500 µg/ml concentration as well as the maximum *in-vitro* total antioxidant activity (60.38%), DPPH activity (58.73%), reducing power effect (52.73%), hydroxyl radical scavenging activity (51.03%) and nitric oxide scavenging activity (45.86%) were recorded at 100 µg/ml concentration of AgNPs with the respective IC_{50} values of 178.9, 52.31, 74.11 89.89 and 155.5 µg/ml. From the results, it could be considered that the biosynthesized AgNPs of *S. olivaceus* (MSU3) has biomedical applications with antibacterial, anti-inflammatory and antioxidant properties.

1. Introduction

Nanotechnology is a fast growing branch of science that deals with synthesis and development of various nano-materials, which are being prepared by copper, zinc, titanium, magnesium, gold, alginate and silver (Husseiny et al., 2015). It is a rapid, upcoming, multidisciplinary promising area that has an influence in medical, food, agricultural, electronic and industrial fields, where they manufacture materials at the nano scale (ranging between 1 and 100 nm in size) (Basavaraj et al., 2012). The nanoparticles can be prepared by employing physical, chemical or biological methods. Generally, the physical method has low yield and the chemical method cause contamination due to precursor chemicals, use of toxic solvents and the generation of hazardous by-products (Wang et al., 2007). Hence, there is a growing need to use eco-friendly, safe, reliable and clean method for the preparation of nanoparticles that does not produce toxic wastes in their process synthesis protocol (Husseiny et al., 2015; Balakumar and Prakash, 2016a).

Silver nanoparticles (AgNPs) are extensively used among all nanomaterials, therefore biological and biomimetic approaches to synthesize silver nanoparticles are under research (Abdel Rahim et al., 2017). AgNPs became the main focus of intensive study because of its wide selection of applications in the areas like catalyst, optics, antimicrobials, anti-oxidants and biomaterial production (Qin et al., 2011; Emmanuel et al., 2017). Biological approaches such as bacteria especially actinobacteria, fungi, yeast and plants can be used for production of nanoparticles like AgNPs, which exhibited different biological activities like antibacterial (Qin et al., 2011), anti-oxidant (Balagurunathan et al., 2011) and anti-cancer (Składanowski et al.,

* Corresponding author.
E-mail address: gimmas@gmail.com (G. Immanuel).

https://doi.org/10.1016/j.bcab.2018.11.014
Received 31 August 2018; Received in revised form 4 November 2018; Accepted 17 November 2018
Available online 19 November 2018
1878-8181/

2017). Among them, actinobacteria are the common source for the synthesis of AgNPs serving as an anti-cancer, anti-oxidant and anti-microbial agent (Składanowski et al. 2017).

Actinobacteria are a cluster of bacteria, which have many important and interesting features. They hold a prominent position due to their diversity and proven ability to produce new compounds like nanoparticles (Das et al., 2008). *Streptomyces* sp is the one of the familiar genus of actinobacteria, efficient producer of valuable bioactive compounds like nanoparticles with wide range of activities (Karthik et al., 2014). Actinobacteria enumerated from various resources have been recognized as the efficient synthesizers of metal nanoparticles (Balagurunathan et al., 2011). Recently, marine sediments are identified as novel sources for identification of actinobacteria, which yield beneficial metabolites such as enzymes, antibiotics and nanoparticles (Sanjivkumar et al., 2018). Nowadays, the biosynthesis of nanoparticles has been reported in few actinobacterial strains such as *Thermomonospora* sp. (Ahmad et al., 2003), *Nocardiopsis* sp. MBRC-1 (Manivasagan et al., 2013), *Rhodococcus* sp. (Ahmad et al., 2003), *Streptomyces viridogens* (HM10) (Balagurunathan et al., 2011), *Nocardia farcinica* (Oza et al., 2012), *S. hygroscopicus*, *Streptomyces* sp. (Karthik et al., 2014), and *S. avidinii* (Park et al., 2006). Considering the usage of actinobacteria, the current investigation was undertaken to biosynthesize AgNPs using a marine actinobacterium, *Streptomyces olivaceus* (MSU3), to characterize the produced AgNPs and also to determine its biomedical potential.

2. Materials and methods

2.1. Experimental strain and inoculum preparation

The experimental strain *Streptomyces olivaceus* (MSU3) with the accession number KM212958 from the marine ecosystem of Southwest coast of India was identified up to species level by standard methods and it was documented in our earlier report (Sanjivkumar et al., 2017). The chosen actinobacterium was further inoculated in a sterile International Streptomyces Project medium − 2 (ISP2) and the culture plate was incubated for 5 days at 28 °C. This culture was elected as working strain for further studies.

50 ml of ISP2 broth was taken in 250 ml Erlenmeyer flask. Then the flask was sterilized at 121 °C for 15 min. The selected culture actinobacterium was inoculated and stored in an incubator at 28 °C for 5 days. After incubation, the biomass was harvested by filtering through Whatman No-1 filter paper and adequately washed with sterile distilled water in order to remove the medium content in the biomass. The collected biomass was further used for the following production studies.

2.2. Biosynthesis of silver nanoparticles

The biosynthesis of silver nanoparticles was performed by using the method of Abd-Elnaby et al. (2016) with minor modification. 10 g (wet weight) of actinobacterial biomass was taken in a 100 ml Erlenmeyer flask containing sterile double distilled water and kept in a rotary shaker (120 rpm) at 28 °C for 48 h. Followed by, the cell filtrate was attained by filtering through Whatman No-1 filter paper. Then, 1 mM $AgNO_3$ prepared in 50 ml of Milli-Q water was mixed with 50 ml of the cell filtrate and kept in a rotary shaker at 28 °C in dark condition for 5 days. The cell filtrate without silver nitrate was served as a control.

2.3. Characterization of silver nanoparticles

The bioreduction of silver ions was examined by observing colour change to dark brown. Further it was confirmed and characterized through UV- vis spectrum, FT-IR, SEM, EDX and XRD analysis (Abd-Elnaby et al., 2016).

2.3.1. UV-Visible spectroscopy analysis

The UV-visible absorption spectrum of the biosynthesized AgNPs was performed by using UV-visible spectrophotometer (Techcomp, UV VIS 8500) within the absorbance (λ_{max}) range of 200 – 8000 nm. Further the stability of biosynthesized AgNPs was assessed in varying temperature (25, 30, 35 and 40 °C) and incubation time (5, 10, 20, 30 and 40 min) (Balakumar et al., 2017).

2.3.2. FT-IR analysis

The FT-IR analysis of the biosynthesized AgNPs was performed by preparing KBr discs using Perkin Elmer spectrophotometer (Perkin Elmer model spectrum-I PC) within the absorption range between 4000 and 400 cm^{-1} (Elumalai and Sakthivel, 2013).

2.3.3. Transmission Electron Microscope (TEM) analysis

The appearance of biosynthesized AgNPs was assessed by transmission electron microscopic analysis. In-order to carry out TEM analysis, the biosynthesized silver nanoparticles solution was centrifuged at 10,000 rpm for 20 min and drop coated on to thin glass film. Then, the sample was examined under Transmission Electron Microscope (JEOL JEM-2100) with an accelerating voltage of 80 kV.

2.3.4. Energy dispersive X-ray spectroscopy (EDX) analysis

The presence of elemental silver of the biosynthesized AgNPs was confirmed through Energy-dispersive X-ray spectroscopy analysis using EDX unit (JEOL JFSM 6390) coupled with transmission electron microscope (TEM).

2.3.5. X-ray diffraction (XRD) analysis

The crystalline metallic nature of the biosynthesized AgNPs was studied through X-ray diffraction method using X-ray diffractometer (X'Pert Pro Analytical Phillips, PW1830) with the 2θ range of 5–120°. The resulted diffractogram was assessed along with standard database like International Centre for Diffraction Data (ICDD).

2.4. Biomedical applications of AgNPs

2.4.1. Antibacterial activity of biosynthesized AgNPs

The clinical human pathogens such as *Streptococcus mutant* (NCIM2063), *S. pneumoniae* (ATCC49619), *Klebsiella pneumoniae* (ATCC10273), *Escherichia coli* (ATCC25922) and *Enterobactor faecalis* (ATCC29212) were acquired from MNP laboratory of CMST, Manonmaniam Sundaranar University. They were individually prepared by using sterile nutrient broth and stored in an incubator for 24 h at 37 °C. Followed by, the individual culture suspensions were used for further studies.

Antibacterial activity of the biosynthesized AgNPs was achieved through agar-well diffusion method by using sterile Muller Hinton (MHA) agar. Wells (5 mm diameter in size) were made with the help of sterile well cutter on MHA. 0.1 ml each of individual pathogenic bacterial strains were spread on the plates, then different concentrations (5, 10, 20 and 30 µl) of the AgNPs (20 µg/ml) were poured in to the wells, simultaneously 25 µg/ml of chloramphenicol was used as positive control. Then the plates were incubated at 37 °C for 24 h and the results were observed (Sanjivkumar et al., 2016).

2.4.2. Determination of MIC and MBC of AgNPs

The MIC of biosynthesized AgNPs against the individual bacterial strains was studied with different concentrations (0.313, 0.625, 1.25, 2.5, 5, 10 and 20 µg/ml). Along with these, 2 ml of sterile nutrient broth was taken in test tubes and 0.1 ml each of bacterial strains were inoculated into the individual tubes. Then the tubes were incubated for 24 h at 37 °C. Simultaneously, Chloramphenicol (25 µg/ml) was used as control. After incubation, the tubes were examined for turbidity. No turbidity in the test tubes has least concentration of AgNPs expressed as MIC. In MBC analysis of the AgNPs, 0.1 ml each of the broth from the

individual culture tubes were gathered and streaked on sterile nutrient agar plates. Simultaneously the plates were stored at 37 °C for 24 h. Followed by no bacterial growth in the least concentration of AgNPs was observed and it was expressed as MBC. All the tests were accessed in triplicate assays

2.4.3. In-vitro anti-inflammatory activity of AgNPs

Anti-inflammatory activity of the biosynthesized AgNPs was achieved through protein denaturation method described by Chandra et al. (2012) with minor modification. In various test tubes, 2 ml each of different concentrations (100 − 500 µg/ml) of AgNPs were taken. To this 2.8 ml of acetate buffered saline (pH 7.0) and 2 ml of egg albumin (from fresh hen's egg) were added and incubated at 28 °C for 15 min. Instead of egg albumin, 100 µg/ml of diclofenac sodium was used as control. The reaction was induced by keeping the tubes in a water bath at 70 °C for 10 min. Finally, the absorbance was measured at 660 nm using a UV-vis spectrophotometer (UV2301II model). The percentage inhibition of protein denaturation was measured by the following formula

$$\text{Inhibition (\%)} = [(A_t - A_c)/A_c] \times 100$$

Where A_t = absorbance of test sample; A_c = absorbance of control (diclofenac sodium)

2.4.4. Determination of antioxidant properties of AgNPs

The synthesized AgNPs at various concentrations (12.5, 25, 50 and 100 µg/ml) were examined for their biomedical efficiency through various assays like *in-vitro* total antioxidant, DPPH, total reducing power, hydroxyl radical and nitric oxide scavenging activities respectively compared with suitable standards.

2.4.4.1. In-vitro total antioxidant activity. The reaction mixture contained 0.1 ml each of various concentrations (12.5, 25, 50, 75 and 100 µg/ml) of AgNPs with 1.9 ml of solution containing 0.6 M sulfuric acid, 28 mM sodium phosphate and 4 mM ammonium molybdate. Then, the reaction mixture was incubated in a water bath at 95 °C for 90 min. After cooling, the optical density of all the samples was measured at 695 nm. From the standard graph of ascorbic acid, the total antioxidant activity was measured by ascorbic acid equivalents in µg/ml of AgNP's dry weight. Butylated hydroxy anisole (BHA) was used as standard antioxidant (Raghava Rao and Raghava Rao, 2013).

2.4.4.2. Total reducing power assay. The total reducing power (TRP) of biosynthesized AgNPs was performed as per the modified method of Yen and Duh (1993). The reaction solution contained various concentrations (12.5, 25, 50 and 100 µg/ml) of AgNPs with 2.5 ml of sodium acetate buffer (0.2 M, pH 7.0) and 2.5 ml of 1% potassium ferric cyanide. Then, the mixtures were boiled at 60 °C for 10 min. After cooling, 2.5 ml of TCA was added and centrifuged at 2000 rpm for 10 min. Then, 1 ml of distilled water along with 250 ml of 0.1% ferric chloride were added to the collected supernatant. Followed by, the optical density was read at 700 nm. The TRP of the AgNPs was measured through the formula

$$\text{Reducing power (\%)} = [(A_{test}/A_{blank}) - 1] \times 100$$

2.4.4.3. DPPH scavenging assay. The DPPH scavenging activity of biosynthesized AgNPs was performed by using 2,2-Diphenyl-1-picrylhydrazyl assay (Chang and Kim, 2001). The reaction solution contained various concentrations (12.5, 25, 50 and 100 µg/ml) of AgNPs, which was made up to 40 ml with DMSO, followed by 2.96 ml of DPPH (0.1 mM) was added. Then the reaction solution was stored in an incubator at room temperature for 30 min under dark condition. Followed by, the optical density of the reaction mixture was measured at 517 nm. DPPH (3.0 ml) alone was considered as control. The scavenging activity was determined through the equation

$$\text{Inhibition (\%)} = [(\text{Control} - \text{Test})/\text{Control}] \times 100$$

2.4.4.4. Hydroxyl radical scavenging assay. The reaction mixture contained EDTA (0.1 ml), $FeCl_3$ (0.01 ml), H_2O_2 (0.1 ml), deoxyribose (0.36 ml) and AgNPs (1.0 ml) with various concentrations (12.5, 25, 50 and 100 µg/ml). Followed by, 0.33 ml of 50 mM of phosphate buffer (pH 7) and 0.1 ml of ascorbic acid were added to the reaction mixture and stored at room temperature for 1 h. About 1.0 ml portion of the incubated mixture was taken in a test tube. To this 1.0 ml of (10%) TCA and 1.0 ml of (0.5%) TBA were added. Pink colour was developed and sequentially the intensity of pink colour was measured at 532 nm (Parejo et al., 2000). The absence of AgNPs in the reaction solution was served as control. Then the scavenging activity of the AgNPs was determined by the following equation

$$\text{Inhibition (\%)} = \frac{\text{Absorbance of control} - \text{Absorbance of standard}}{\text{Absorbance of control}} \times 100$$

2.4.4.5. Nitric oxide scavenging activity. The nitric oxide scavenging activity of the AgNPs was performed through the method of Green et al. (1982). The reaction solution contained AgNPs (0.5 ml) with various concentrations (12.5, 25, 50 and 100 µg/ml) and sulphosalicylic acid (0.1 ml). Further the reaction solution was vortexed for 25 min. Then it was centrifuged at 6000 rpm for 10 min. Followed by, 30 µl of 10% NaOH and 300 µl of Tris-HCl buffer were added to 200 µl of collected supernatant solution and vortexed well. Along with this, 530 µl of Griess reagent was added and stored for 20 min in an enclosed condition. Finally, it was measured (546 nm) using Griess reagent as blank. The reaction mixture without the AgNPs was acted as control. The nitric oxide scavenging activity of AgNps was assessed by the following equation

$$\text{Inhibition (\%)} = [(\text{Control} - \text{Test})/\text{Control}] \times 100$$

2.5. Statistical analysis

The data obtained in this investigation were expressed as Mean ± SD and were analyzed using One – Way ANOVA test and subsequently conducted *post hoc* multiple comparison with SNK test at 5% level of significance using computer software STATISTICA 6.0 (Statosoft, Bedford, UK).

3. Result and discussion

Biological synthesis of nanoparticles mediated by actinobacteria has vast range for developing nanoantimicrobials or nanoantibiotics which could be served as alternative therapeutic agents with various biological applications (Manivasagan et al., 2015). In view of this, in the current investigation, a marine bacterium *S. olivaceus* (MSU3) from southwest coast of India was employed for production of silver nanoparticles (AgNPs) in laboratory condition and the proposed mechanism of biosynthesis of AgNPs using *S. olivaceus* (MSU3) is shown in Fig. 1. Further the produced AgNPs was characterized and also its biomedical properties were assessed.

3.1. Characterization of AgNPs

3.1.1. UV-visible spectroscopy analysis

In the present investigation, the UV-visible spectral analysis of synthesized AgNPs of the experimental actinobacterium *S. olivaceus* (MSU3) was achieved with a maximum peak at the absorption range 450 nm (Fig. 2). The formation of metallic nano silver was gradually increased at the temperature ranged from 25° to 40°C with the incubation time of 5–60 min respectively, and the biosynthesized AgNPs was maximally attained at 40 °C for 60 min (Fig. 3a & b) by the

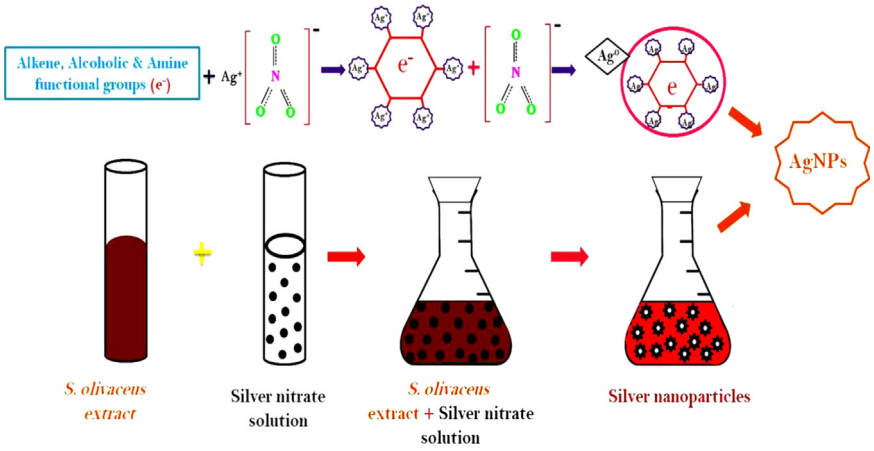

Fig. 1. Schematic diagram of the possible bio-reduction process involved in the AgNPs synthesis.

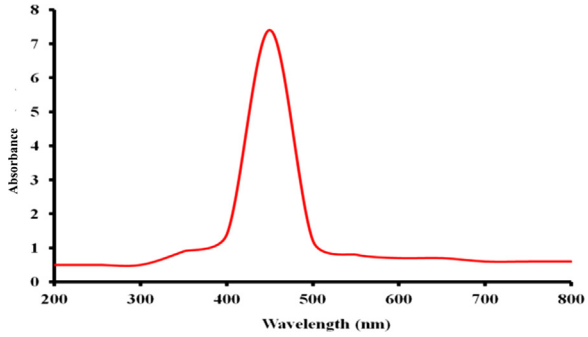

Fig. 2. UV- visible spectral analysis of AgNPs from *S. olivaceus* (MSU3).

reductive molecules of silver ions from silver nitrate solution. Likewise, Balakumar et al. (2017) reported the AgNPs from *Madhuca longifolia* expressed highly intense peak with a maximum absorbance at 442 nm within the reaction time of 110 min under UV-visible spectroscopy analysis. Wypij et al. (2018) documented the AgNPs from *Streptomyces xinghaiensis* (OF1) exhibited narrow peak with a maximum absorbance (420 nm) at 40 °C under UV-visible spectroscopy analysis. Manikprabhu and Lingappa (2013) performed the UV-Vis spectral analysis of AgNPs of *S. coelicolor* showed the maximum absorption range between 450 and 400 nm. Similarly, Sivalingam et al. (2012) reported the AgNPs of *Streptomyces* sp BDUKAS10 from marine mangrove sediment showed the maximum peak range from 424 to 404 nm. Husseiny et al. (2015) attained the maximum (420 nm) peak range of biosynthesized AgNPs of *Fusarium oxysporum* using UV-visible spectroscopy.

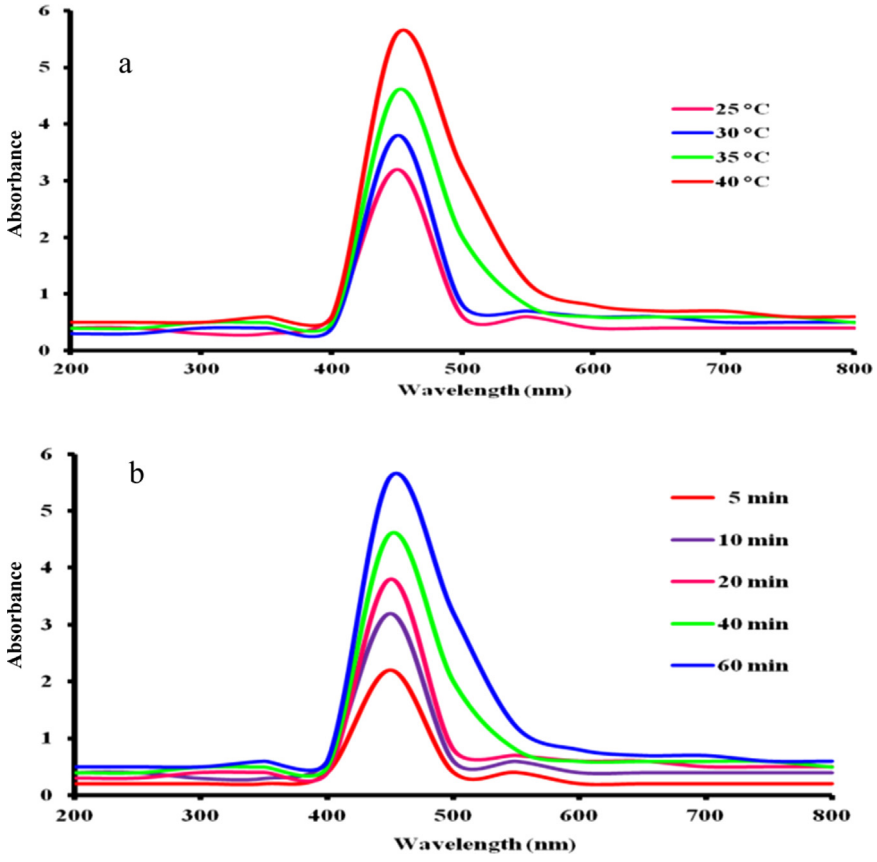

Fig. 3. Determination of the stability of AgNPs from *S. olivaceus* (MSU3) through UV- Vis spectra at different temperature (a) and time intervals (b).

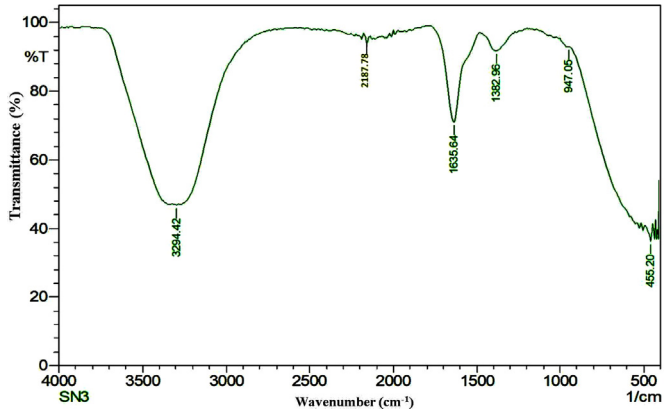

Fig. 4. FT-IR analysis of AgNPs from *S. olivaceus* (MSU3).

3.1.2. FT-IR analysis

In FT-IR analysis, totally 5 major functional groups were found in between the wave number range between 455.20 and 3294.42 cm^{-1}. The alkyne (C=C-H) and alcohol (ROH) groups were predominantly found at the wave number range of 455.20 – 3.294.42 cm^{-1} with stretchable and strong intensity (Fig. 4). Followed by, oxime (C=N-OH), alkene (C-C), carboxyl (RCOOH) and amine (R-NH_2)groups were noticed at the wave number of 957.05, 1382.96, 1635.64 and 2187.78 cm^{-1} respectively with bend and weak intensity. Similarly, Wypij et al. (2018) determined the characterization of biosynthesized AgNPs of *S. xinghaiensis* (OF1) under FT-IR analysis showed five functional groups (N-H, C-H, C=C, -C-H, C-O) with the respective peak ranges of 3432, 2925, 1631, 1385 and 1033 cm^{-1}. Skladanowski et al. (2017) achieved the characterization of AgNPs from *Streptomyces* sp. which exhibited seven groups (C=O, C-H, C=N, C-O, C-Cl, N-H and C=C) in between the wavenumber range of 3447 – 875 cm^{-1}. Abd-Elnaby et al. (2016) reported the AgNPs of *S. rocheii* (MHM13) exhibited seven functional groups (N-H, C-H, O=C=O, C=C, -C-H, C-O and C-Cl or C-Br) in between the wavenumbers of 3420.14 and 613.25 cm^{-1} using FT-IR.

3.1.3. Transmission electron microscopic analysis

The TEM analysis was performed to describe the shape and size of the silver nanoparticles biosynthesized by *S. rocheii* (MHM13) expressed spherical in shape with the size range from 22 to 85 nm (Abd-Elnaby et al., 2016). In the present investigation, particle size of the synthesized AgNPs from *S. olivaceus* (MSU3) was achieved by TEM analysis, which articulated the morphology of the monodisperse AgNPs, is almost spherical in shape with the particle size of 12.3 nm (Fig. 5). Likewise, Sivasankar et al. (2018) reported the transmission electron microscopic analysis of AgNPs of *S. violaceus* (MM72) revealed spherical shape ranging from 10 to 60 nm. In an another study, the TEM image of AgNPs of *S. coelicolor* expressed irregular shape having the size range of 20 – 50 nm was reported by Manikprabhu and Lingappa (2013). Deepa et al. (2013) documented the size and shape of biosynthesized AgNPs from marine actinobacteria *Thermoactinomycetes* sp showed the size range of 20 – 40 nm with spherical in shape under SEM analysis.

3.1.4. Energy dispersive x-ray spectroscopic analysis

Energy dispersive x-ray spectroscopy (EDX) is very helpful to provide elemental or chemical characterization of nanoparticles by measuring energy and intensity of x-rays (Abd-Elnaby et al., 2016; Balakumar and Prakash, 2016b). In the present investigation, the presence of elemental silver component in the biosynthesized AgNPs of *S. olivaceus* (MSU3) was detected through EDX analysis and the result indicated the presence of Ag, Cu and C groups with the atomic weight of 8.08%, 3.65% and 88.27% respectively (Fig. 6), it shows the EDX pattern of AgNps which confirms the existence of Ag elements with strong signal (3 keV) at silver region, which proves the formation of elemental silver by the reduction of silver ions. Likewise, In accordance with these Hebeish et al. (2014) stated that the atomic weight of Ag (6.26%), Cl (2.92%) and O (89.21%) were observed within the spectrum appeared around 3 keV indicated the existence of elemental silver in the biosynthesized AgNPs of *Streptomyces* sp. Skladanowski et al. (2017) documented the EDX analysis of AgNPs of *Streptomyces* sp showed elemental Ag (6.52%), C (82.8%) and O (98.2%). Likewise, EDX analysis of elemental composition like C (47.5%), O (34.37%), Ca (1.17%), K (0.08%), Zn (4.48%) and Si (8.19%) of nanocatalyst of *Streptomyces* sp were reported by Bharati and Suresh (2017).

3.1.5. X-ray diffraction study

X-ray diffraction (XRD) study revealed the crystalline nature of the particles and the XRD pattern obtained is shown in Fig. 7. It showed four intense peaks in the whole spectrum of 2θ peak values around 38.12°, 44.30°, 64.45° and 77.41° indexed at the lattice plane (111), (200), (220) and (311) respectively. All the obtained peaks were analyzed through the Joint Committee on Powder Diffraction Standards (JCPDS) data with the No. 044387. According to Debye-Scherrer equation ($D = k\lambda/\beta\cos\theta$), the average size of the biosynthesized AgNPs was found to be approximately 12.3 nm. In an another study, Balakumar and Prakash (2016c) documented the diffraction peaks at 2θ values (37.89°, 44.63°, 64.72° and 77.69°) with the lattice plane (111), (200), (220) and (311) of crystalline AgNPs from *Bombax ceiba* were assessed by XRD analysis with the JCPDS No 040783. Likewise, Skladanowski et al. (2017) achieved the XRD analysis of biosynthesized AgNPs of *Streptomyces* sp showed six intense peaks with 2θ values of 38.1°, 44.6°, 64.6°, 77.5°, 81.5° and 115.0°. Sivasankar et al. (2018) performed XRD analysis of AgNPs from *S. violaceus* (MM72) revealed four strong silver peaks in the spectrum with 2θ values ranging from 30° to 80°. XRD intense peak values [38.15° (111), 44.18° (200), 64.63° (220) and 77.50° (311)] of AgNPs from *Fusarium oxysporum* were described by Husseiny et al. (2015). Manikprabhu and Lingappa (2013) documented the XRD pattern of AgNPs of *S. coelicolor* expressed with the peak values of 40.21° and 75.41°.

3.2. Antibacterial activity of AgNPs by agar well diffusion method

In this investigation, the antibacterial efficiency of the synthesized AgNPs was studied and the result is documented (Table 1). It expressed that the AgNP from the candidate strain MSU3 exhibited the highest (23.0 mm) inhibition against *S. pneumoniae* at 30 µl concentration and the minimum inhibition of 16.0 mm was observed at 5 µl concentration. At the same time, *S. mutant* expressed the maximum zone of inhibition (22.0 mm) at 30 µl concentration and the minimum inhibition (15.0 mm) at 5 µl concentration. Another test pathogen of this investigation, *K. pneumoniae* displayed the highest zone of inhibition of 16.0 mm, which was observed at 30 µl concentration, and the minimum inhibition (12.0 mm) at 20 µl concentration. The strain *E. coli* exhibited the maximum zone of inhibition (16.0 mm) at 30 µl concentration. The same pathogen attained the zone of inhibition of 0.00, 9.00 and 13.0 mm at 5, 10, and 20 µl concentrations, respectively. All the results were respectively compared with the positive control (i.e. Chloramphencol), which expressed the zone of inhibition from 16.0 to 18.0 mm at the concentration of 20 µg/ml. Similarly, Abd-Elnaby et al. (2016) reported the antibacterial activity of AgNPs of marine actinobacterium *S. rocheii* MHM13 through agar-well diffusion assay, it expressed the growth inhibition against *B. subtilis* (18.0 mm), *S. aureus* (18.0 mm) and *V. fluvialis* (19.0 mm). In an another study, the extracellular AgNPs from *S. parvulus* SSNP11 exhibited the zone of inhibition of 30.0, 26.0, 21.0 and 26.0 mm against the pathogens such as *B. subtilis*, *S. typhi, P. putida* and *K. pneumoniae* respectively were documented by Prakasham et al. (2014). Sivalingam et al. (2012) studied the antibacterial activity of biosynthesized AgNPs of *Streptomyces* sp

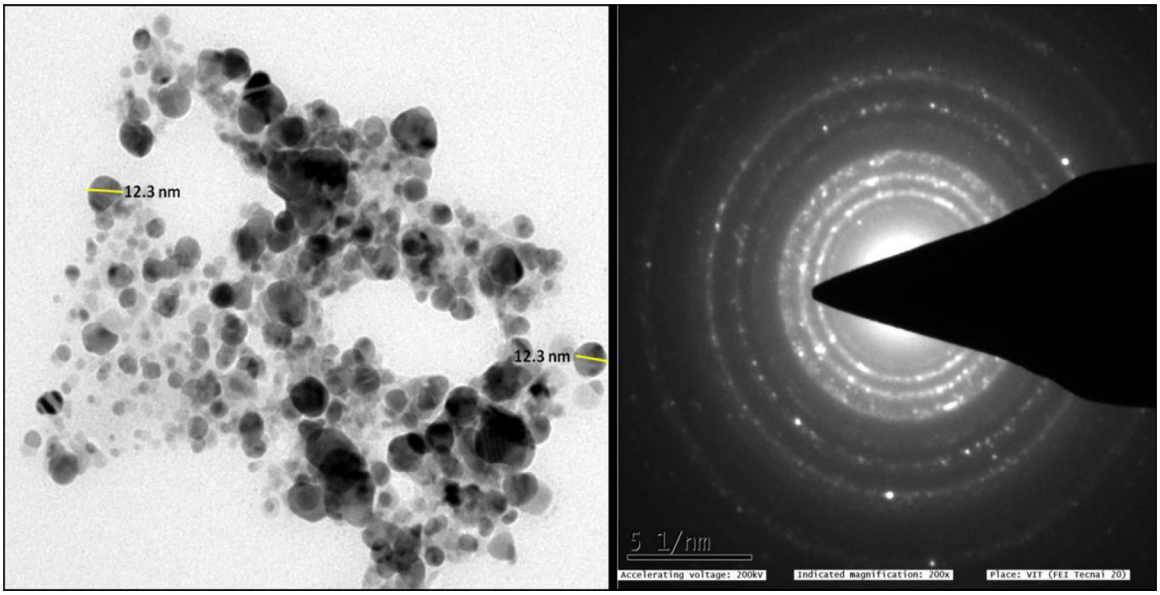

Fig. 5. Transmission Electron Microscopic analysis of AgNPs from *S. olivaceus* (MSU3).

BDUKAS10 showed the zone of inhibition of 16.0 mm against *S. aureus*, 15.0 mm against *P. aeruginosa* and 13.0 mm against *B. cereus*. Saravanan et al. (2018) reported the maximum growth inhibition of AgNPs from *B. brevis* (NCIM 2533) against *S. aureus* (19.0 mm) under laboratory condition through agar well diffusion method.

3.2.1. MIC and MBC of biosynthesized AgNPs

The biosynthesized AgNPs of this study exhibited highest activity against *S. pneumoniae* with 0.625 and ≤ 2.50 µg/ml of MIC and MBC respectively, when compared to the positive control chloramphenicol (20 µg/ml). It also expressed the MIC and MBC values against the other tested clinical pathogens such as *S. mutant* (0.625 and ≤ 5.00 µg/ml), *K. pneumoniae* (2.50 and ≥ 5.00 µg/ml), *E. coli* (1.25 and ≤ 5.00 µg/ml) and *E. faecalis* (1.25 and ≤ 2.50 µg/ml) (Table 2). Similarly, Wypij et al. (2018) observed the MIC of AgNPs produced by *S. xinghaiensis* (OF1) had 16 µg/ml against *P. aeruginosa* and 32 µg/ml against *Candida albicans* with the highest MBC values recorded against *P. aeruginosa* (32 µg/ml) and *E. coli* (64 µg/ml). Skladanowski et al. (2017) achieved

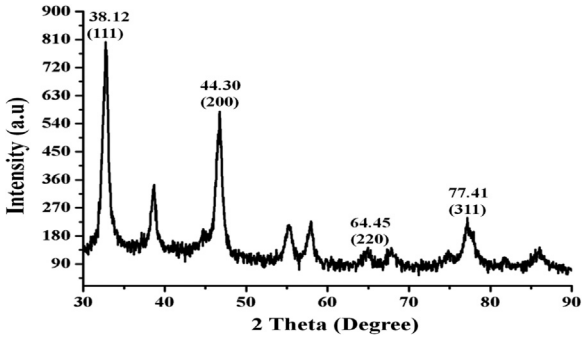

Fig. 7. X-ray Diffraction analysis of AgNPs from *S. olivaceus* (MSU3).

the highest MIC values of AgNPs of *Streptomyces* sp expressed 5 µg/ml against *K. pneumoniae*, 10 µg/ml each against *P. aeruginosa* and *B. subtilis*. Also they recorded that the highest MBC values against *P.*

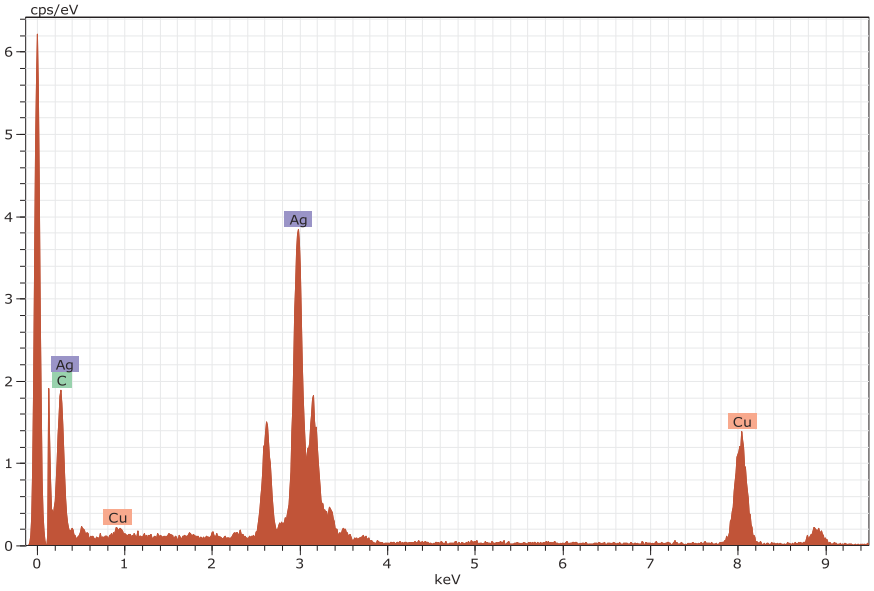

Fig. 6. Energy dispersive X-ray spectroscopy of AgNPs from *S. olivaceus* (MSU3).

Table 1
Antibacterial activity of AgNPs from *S. olivaceus* (MSU3) against human clinical pathogens.

Conc. of AgNPs (µl)	Clinical pathogens				
	Zone of inhibition (mm)				
	S. mutant	*S. pneumoniae*	*K. pneumonia*	*E. coli*	*E. faecalis*
5	15.0 ± 1.63	16.0 ± 1.52	0.00 ± 0.00	0.00 ± 0.00	10.0 ± 1.49
10	18.0 ± 1.64	18.0 ± 1.59	0.00 ± 0.00	9.00 ± 1.30	12.0 ± 1.57
20	19.0 ± 1.65	20.0 ± 1.60	12.0 ± 1.57	13.0 ± 1.55	14.0 ± 1.61
30	22.0 ± 1.62	23.0 ± 1.64	16.0 ± 1.60	16.0 ± 1.57	17.0 ± 1.63
Positive control (Chloramphenicol 20 µg/ml)	17.0 ± 1.62	16.0 ± 1.60	18.0 ± 1.64	17.0 ± 1.66	18.0 ± 1.58

Each value is the Mean ± SD of triplicate analysis.

Table 2
Determination of MIC and MBC of AgNPs of *S. olivaceus* (MSU3) against human clinical pathogens.

Clinical pathogens	MIC (µg/ml)	MBC (µg/ml)
S. mutant	0.625	≤ 5.00
S. pneumoniae	0.625	≤ 2.50
K. pneumoniae	2.50	≥ 5.00
E. coli	1.25	≤ 5.00
E. faecalis	1.25	≤ 2.50

aeruginosa (140 µg/ml) and *B. subtilis* (170 µg/ml). The MIC values of AgNPs of *S. kasugaensis* M338-M1 against *B. subtilis* (2.5 µg/ml), *P. aeruginosa* (10 µg/ml), *S. aureus* (1.25 µg/ml) and *S. infantis* (10 µg/ml) were stated by Skladanowski et al. (2016). Manikprabu and Lingappa (2013) reported the highest MIC and MBC values of AgNPs from *S. coelicolor* expressed 30 and 40 µg/ml respectively against multidrug resistant *S. aureus*.

3.3. Anti-inflammatory activity of biosynthesized AgNPs

In the present investigation, the anti-inflammatory activity of AgNPs at various concentrations (100, 200, 300, 400 and 500 µg/ml) from the candidate strain showed the inhibition percentage of 28.76%, 49.32%, 71.64%, 87.32% and 97.53% along with the IC_{50} value of 178.9 µg/ml (Table 3). Which expressed the increasing concentration of AgNPs (100–500 µg/ml) influences the inhibition percentage, whereas inhibition percentage of the standard diclofenac sodium expressed 89.21% with 170.0 µg/ml of IC_{50} value. Similarly, Govindappa et al. (2016) stated the anti-inflammatory efficiency of biosynthesized AgNPs from *Penicillium* sp expressed the highest percentage inhibition (85.92%) at 200 µl concentration. Likewise, Sriramulu and Sumathi (2017) stated a maximum percentage inhibition of 84.0% at 200 µl concentration of AgNP of *Ganoderma lucidium* under laboratory condition. Hebeish et al. (2014) documented the anti-inflammatory effect of colloidal solution of AgNPs showed the highest percentage inhibition (55.90%) at 250 ppm concentration.

3.4. Antioxidant properties of biosynthesized AgNPs

Antioxidants neutralize free radicals thereby protecting cell damage and to play a significant role in biomedical applications (Hamasaki et al., 2008). Sreedevi et al. (2015) studied the total antioxidant property of AgNPs of *Monostroma oxyspermum* showed the maximum activity range from 33.2% to 66.29% at 50–250 µg/ml concentrations. In the present investigation, the total antioxidant property of the synthesized AgNPs was tested by using five different assays and the results are presented in Table 3. In *in-vitro* antioxidant property, the AgNPs expressed highest (60.38%) inhibition at 100 µg/ml concentration, while lowest (28.0%) inhibition was observed at 12.5 µg/ml concentration. In DPPH scavenging activity, the AgNPs exhibited increased inhibition percentage (36.12%, 41.87%, 47.00% and 58.73%) with the increasing concentrations (12.5, 25, 50 and 100 µg/ml) of AgNPs with the IC_{50} value of 52.31 µg/ml. In reducing power assay, the AgNPs expressed the maximum percentage inhibition (52.73%) at 100 µg/ml concentration, but the minimum (22.08%) at 12.5 µg/ml concentration along with 74.11 µg/ml of IC_{50} value (Fig. 8).

In hydroxyl radical scavenging activity, the synthesized AgNPs of *S. olivaceus* exhibited the highest percentage inhibition of 51.03% at 100 µg/ml concentration and the lowest (12.09%) inhibition was noticed at the concentration of 12.5 µg/ml with 89.89 µg/ml of IC_{50} value. The nitric oxide scavenging activity of AgNPs of *S. olivaceus* showed the percentage inhibition of 18.34%, 24.52%, 35.22% and 45.86% at 12.5, 25, 50 and 100 µg/ml concentrations respectively with the IC_{50} value of 155.5 µg/ml (Fig. 8). Similarly, Sivasankar et al. (2018) documented the antioxidant properties of biosynthesized AgNPs from *S. violaceus* (MM72), who stated the maximum scavenging activity of 73.0% for *in-vitro* total antioxidant, 89.5% for DPPH, 72.5% for hydroxyl radical scavenging assay, 60.1% for nitric oxide scavenging assay at the respective concentration of 50 µg/ml. Shanmugasundaram et al. (2013) documented the antioxidant efficiency of AgNPs from *S. naganishii* (MA7), which had the maximum scavenging activity of 80% for nitric

Table 3
Determination of *In-vitro* anti-inflammatory and total antioxidant activities of AgNPs from *S. olivaceus* (MSU3).

Conc. of AgNPs (µg/ml)	*In-vitro* anti-inflammatory activity		Conc. of AgNPs (µg/ml)	*In-vitro* total antioxidant activity	
	(%) Inhibition	IC_{50} (µg/ml)		(%) Inhibition	IC_{50} (µg/ml)
100	28.76 ± 1.39[a]	178.9 ± 1.90	12.5	28.00 ± 1.29[a]	51.86 ± 1.45
200	49.32 ± 1.66[b]		25	35.08 ± 1.59[b]	
300	71.64 ± 1.76[c]		50	48.21 ± 1.64[c]	
400	87.32 ± 1.73[d]		75	54.33 ± 1.67[d]	
500	97.53 ± 1.59[e]		100	60.38 ± 1.45[e]	
Diclofenac sodium	89.21 ± 1.67[d]	170.0 ± 1.72	BHA*	57.06 ± 1.56[d]	49.10 ± 1.45

Each value is the Mean ± SD of triplicate analysis, within each column of individual groups, means with different superscript letters are statistically significant (One-way ANOVA test: $P < 0.05$; further *post hoc* multiple comparison with SNK test).
* Butylated hydroxy anisole.

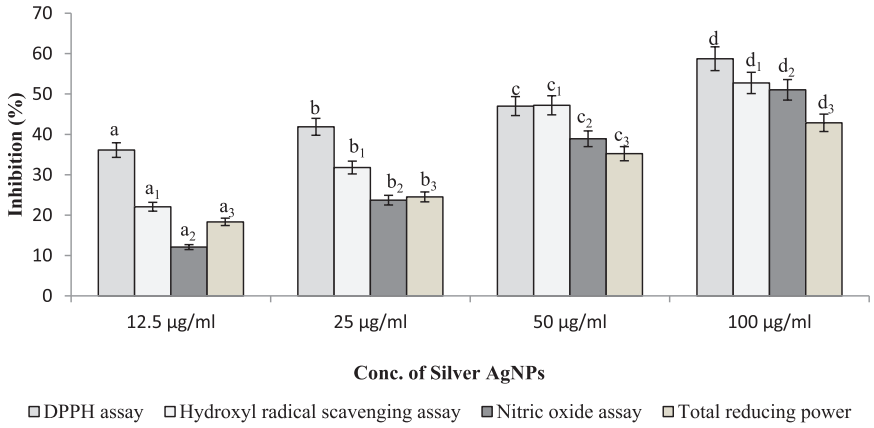

Fig. 8. Different antioxidant assays of AgNPs from *S. olivaceus* (MSU3). Each value is the Mean ± SD of triplicate analysis, individual group of bars represented with different superscript letters are statistically significant (One-way ANOVA test: $P < 0.05$; further *post hoc* multiple comparison with SNK test).

oxide and 75% for hydroxyl radical scavenging assay at 500 µl concentration. The AgNPs of *Solanum torvum* exhibited the highest scavenging activity of DPPH (57.0%), hydroxyl radicals (50.0%), nitric oxide (53.11%) and super oxide (52.0%) scavenging activities at 100 µg/ml concentration were attained by Ramamurthy et al. (2013).

4. Conclusion

From this investigation, it could be concluded that the experimental strain *S. olivaceus* (MSU3) from marine ecosystem was effectively synthesized AgNPs. The produced AgNPs was characterized through UV-visible spectroscopy, FT-IR, TEM, EDX and XRD analysis, which expressed spherical in shape with the average size of around 12.3 nm. The biosynthesized AgNPs was highly inhibited the growth of human clinical pathogens, which exhibited maximum inhibition against *S. pneumoniae* (23 mm) at the highest concentration (30 µl) along with 0.625 and ≤ 2.50 µg/ml of MIC and MBC respectively. Further, it was determined that the AgNPs has biomedical properties, especially as anti-inflammatory and antioxidant agent.

Acknowledgment

The authors gratefully acknowledge the University Grants Commission (UGC), New Delhi, Govt. of India, for its financial support in the form of Special Assistance Programme (SAP) [UGC No. F.3–24/2012(SAPII)dtd October 2012]. The authors thank the Management and the Principal of K.R. College for their moral support.

References

Abdel Rahim, K., Mahmoud, S.Y., Mohamed Ali, A., Almaary, K.S., Mustafa, M.A., Moussa, S., 2017. Extracellular biosynthesis of silver nanoparticles using *Rhizopus stolonifer*. Saudi J. Biol. Sci. 24, 208–216.

Abd-Elnaby, H.M., Abo-Elala, G.M., Abdel-Raouf, U.M., Hamed, M.M., 2016. Antibacterial and anticancer activity of extracellular synthesized silver nanoparticles from marine S*treptomyces rocheii* MHM13. Egypt. J. Aquat. Res. 42, 301–312.

Ahmad, A., Mukherjee, P., Senapati, S., Mandal, D., Khan, M.I., Kumar, R., Sastry, M., 2003. Extracellular biosynthesis of silver nanoparticles using the fungus *Fusarium oxysporum*. Colloids Surf. B Biointerfaces 28, 313–318.

Balagurunathan, R., Radhakrishnan, M., Rajendran, R.B., Velmurugan, D., 2011. Biosynthesis of gold nanoparticles by actinomycetes *Streptomyces viridogens* strain HM10. Indian J. Biochem. Biophys. 48, 331–335.

Balakumar, V., Prakash, P., 2016a. A facile, one-pot and eco-friendly synthesis of gold/silver nanobimetallics smartened rGO for enhanced catalytic reduction of hexavalent chromium. RSC Adv. 6, 57380–57388.

Balakumar, V., Prakash, P., 2016b. Silver nanoparticles embedded RGO-nanosponge for superior catalytic activity towards 4-nitrophenol reduction. RSC Adv. 6, 88837–88845.

Balakumar, V., Prakash, P., 2016c. Green synthesized nanospherical silver for selective and sensitive sensing of Cd^{++} colorimetrically. RSC Adv. 6, 35778–35784.

Balakumar, V., Prakash, P., Muthupandi, K., Rajan, A., 2017. Nanosilver for selective and sensitive sensing of saturnism. Sens. Act. B. 241, 814–820.

Basavaraj, U., Praveenkumar, N., Sabiha, T.S., Rupali, S., Samprita, B., 2012. Synthesis and characterization of silver nanoparticles. Int. J. Pharm. Biol. Sci. 3, 10–14.

Bharati, R., Suresh, S., 2017. Biosynthesis of ZnO/SiO_2 nanocatalyst with palash leaves powder for treatment of petroleum refinery effluent. Resour. Effic. Technol. 3, 528–541.

Chandra, S., Chatterjee, P., Deyand, P., Bhattacharya, S., 2012. Evaluation of *in vitro* anti-inflammatory activity of coffee against the denaturation of protein. Asian Pac. J. Trop. Biomed. 24, 178–180.

Chang, H.B., Kim, J.H., 2001. Antioxidant properties of Dihydro herbimycin – a from a newly isolated *Streptomyces* sp. Biotechnol. Lett. 29, 599–603.

Das, S., Lyla, P.S., Khan, S.A., 2008. Distribution and generic composition of culturable marine actinomycetes from the sediments of Indian continental slope of Bay of Bengal. Chin. J. Oceanol. Limnol. 26, 166–177.

Deepa, S., Kanimozhi, K., Panneerselvam, A., 2013. Antimicrobial activity of extracellularly synthesized silver nanoparticles from marine derived actinomycetes. Int. J. Curr. Microbiol. Appl. Sci. 2, 223–230.

Elumalai, S., Sakthivel, R., 2013. GC-MS and FT-IR spectroscopic determination of fatty acid methyl ester of 16 fresh water microalgae, isolated from cement industries of TamilNadu, India. J. Algal Biomass-. Utln. 4, 50–69.

Emmanuel, R., Saravanan, M., Ovais, M., Padmavathy, S., Shinwari, Z., Prakash, P., 2017. Antimicrobial efficacy of drug blended biosynthesized colloidal gold nanoparticles from J*usticia glauca* a*gainst* oral pathogens: a nanoantibiotic approach. Microb. Pathog. 113, 295–302.

Govindappa, M., Farheen, H., Chandrappa, C.P., Channabasava, P., Rai, R.V., Raghavendra, V.B., 2016. Mycosynthesis of silver nanoparticles using extract of endophytic fungi, Penicillium species of *Glycosmis mauritiana,* and its antioxidant, antimicrobial, anti-inflammatory and tyrokinase inhibitory activity. Adv. Nat. Sci. Nanosci. Nanotech. 7, 1–9.

Green, L.C., Wagner, D.A., Glogowski, J., Tannenbaum, S.R., 1982. Analysis of nitrate and 15N nitrate in biological fluids. Anal. Biochem. 126, 131–136.

Hamasaki, T., Kashiwagi, T., Imada, T., Nakamichi, N., Aramaki, S., Toh, K., Morisawa, S., Shimakoshi, H., Hisaeda, Y., Shirahata, S., 2008. Kinetic analysis of superoxide anion radical scavenging and hydroxyl radical scavenging activities of platinum nanoparticles. Langmuir 24, 7354–7364.

Hebeish, A., El-Rafiea, M.H., EL-Sheikha, M.A., Seleemb, A.A., El-Naggara, M.E., 2014. Antimicrobial wound dressing and anti-inflammatory efficacy of silver nanoparticles. Int. J. Biol. Macromol. 65, 509–515.

Husseiny, S.M., Salah, T.A., Anter, H.A., 2015. Biosynthesis of size controlled silver nanoparticles by *Fusarium oxysporum,* their antibacterial and antitumor activities. J. Basic Appl. Sci. 4, 225–231.

Karthik, L., Kumar, G., Vishnu Kirthi, A., Rahuman, A.A., Rao, K.V.B., 2014. *Streptomyces* sp. LK3 mediated synthesis of silver nanoparticles and its biomedical application. Bioprocess Biosyst. Eng. 37, 261–267.

Manikprabhu, D., Lingappa, K., 2013. Antibacterial activity of silver nanoparticles against methicillin-resistant *Staphylococcus aureus* synthesized using model *Streptomyces* sp. pigment by photo-irradiation method. J. Pharm. Res. 6, 255–260.

Manivasagan, P., Venkatesan, J., Senthilkumar, K., Sivakumar, K., Kim, S.K., 2013. Biosynthesis, antimicrobial and cytotoxic effect of silver nanoparticles using a novel N*ocardiopsis* sp. MBRC-1. BioMed. Res. Int. 13, 1–9.

Manivasagan, P., Alam, M.S., Kang, K., Kwak, M., Kim, S., 2015. Extracellular synthesis of gold bionanoparticles by *Nocardiopsis* sp. and evaluation of its antimicrobial, antioxidant and cytotoxic activities. Bioprocess Biosyst. Eng. 38, 1167–1177.

Oza, G., Pandey, S., Gupta, A., Kesarkar, R., Sharon, M., 2012. Biosynthetic reduction of gold ions to gold nanoparticles by *Nocardia farcinica*. J. Microbiol. Biotechnol. Res. 2, 511–515.

Parejo, I., Codina, C., Petrakis, C., Kefalosp, T., 2000. Evaluation of scavenging activity assessed by Co (II) /EDTA induced luminal chemiluminescence and DPPH free radical assay. J. Pharmacol. Toxicol. Methods 44, 507–512.

Park, T.J., Lee, S.Y., Lee, S.J., Park, J.P., Yang, K.S., Lee, K., Ko, S., Park, J.B., Kim, T., Kim, S.K., 2006. Protein nanopatterns and biosensors using gold binding polypeptide as a fusion partner. Anal. Chem. 78, 7197–7205.

Prakasham, R.S., Kumar, B.S., Kumar, Y.S., Kumar, P.K., 2014. Production and characterization of protein encapsulated silver nanoparticles by marine isolate *Streptomyces parvulus* SSNP11. Indian J. Microbiol. 54, 329–336.

Qin, X., Lu, W., Luo, Y., Chang, G., Sun, X., 2011. Preparation of Ag nanoparticle decorated polypyrrole colloids and their application for H_2O_2 detection. Electrochem. Commun. 13, 785–787.

RaghavaRao, K.V., RaghavaRao, T., 2013. Molecular characterization and its antioxidant activity of a newly isolated *Streptomycetes coelicoflavus* BC01 from mangrove soil. J. Young-. Pharm. 5, 121–126.

Ramamurthy, C.H., Padma, M., Daisy mariya samadanam, I., Mareeswaran, R., Suyavaran, A., Suresh Kumar, M., Premkumar, K., Thirunavukkarasu, C., 2013. The extra cellular synthesis of gold and silver nanoparticles and their free radical scavenging and antibacterial properties. Colloids Surf. B Biointerfaces 102, 808–815.

Sanjivkumar, M., RameshBabu, D., Suganya, A.M., Silambarasan, T., Balagurunathan, R., Immanuel, G., 2016. Investigation on pharmacological activities of secondary metabolite extracted from a mangrove associated actinobacterium *Streptomyces olivaceus* (MSU3). Biocatal. Agric. Biotechnol. 6, 82–90.

Sanjivkumar, M., Silambarasan, T., Palavesam, A., Immanuel, G., 2017. Bioconversion and bioethanol production from agro-residues through fermentation process using mangrove associated actinobacterium *Streptomyces olivaceus* (MSU3). Biofuels. https://doi.org/10.1080/759726 9. 2017.1309853.

Sanjivkumar, M., Brindhashini, A., Deivakumari, M., Palavesam, A., Immanuel, G., 2018. Investigation on saccharification and bioethanol production from pretreated agro-residues using a mangrove associated actinobacterium *Streptomyces variabilis* (MAB3). Waste Biomass-. Valor 9, 969–984.

Sreedevi, P., Moovendhan, M., Sudharsan, S., Vasanthkumar, S., Srinivasan, A., Vairamani, S., 2015. Structural characterization and bioactivities of sulfated polysaccharide from *Monostroma oxyspermum*. Int. J. Biol. Macromol. 72, 1459–1465.

Shanmugasundaram, T., Radhakrishnan, M., Gopikrishnan, V., Pazhanimurugan, R., Balagurunathan, R., 2013. A study of the bactericidal, anti-biofouling, cytotoxic and antioxidant properties of actinobacterially synthesised silver nanoparticles. Colloids Surf. B Biointerfaces 111, 680–687.

Sivalingam, P., Antony, J.J., Siva, D., Achiraman, S., Anbarasu, K., 2012. Mangrove *Streptomyces* sp. BDUKAS10 as nanofactory for fabrication of bactericidal silver nanoparticles. Colloids Surf. B Biointerfaces 98, 12–17.

Sivasankar, P., Sreedevi, P., Poongodi, S., Sivakumar, M., Murugan, T., Sivakumar, L., Sivakumar, K., Balasubramanian, T., 2018. Characterization, antimicrobial and antioxidant property of exopolysaccharide mediated silver nanoparticles synthesized by *Streptomyces violaceus MM72*. Carbohydr. Polym. 181, 752–759.

Składanowski, M., Golinska, P., Rudnicka, K., Dahm, H., Rai, M., 2016. Evaluation of cytotoxicity, immune compatibility and antibacterial activity of biogenic silver nanoparticles. Med. Microbiol. Immunol. 205, 603–613.

Składanowski, M., Wypij, M., Laskowski, D., Golinska, P., Dahm, H., Rai, M., 2017. Silver and gold nanoparticles synthesized from *Streptomyces* sp. isolated from acid forest soil with special reference to its antibacterial activity against pathogens. J. Clust. Sci. 28, 59–79.

Sriramulu, M., Sumathi, S., 2017. Photocatalytic, antioxidant, antibacterial and anti-inflammatory activity of silver nanoparticles synthesised using forest and edible mushroom. Adv. Nat. Sci. Nanosci. Nanotech. 8, 1–9.

Wang, Z., Chen, J., Yang, P., Yang, W., 2007. Biomimetic synthesis of gold nanoparticles and their aggregates using a polypeptide sequence. Appl. Organomet. Chem. 21, 645–651.

Wypij, M., Czarnecka, J., Świecimska, M., Dahm, H., Rai, M., Golinska, P., 2018. Synthesis, characterization and evaluation of antimicrobial and cytotoxic activities of biogenic silver nanoparticles synthesized from *Streptomyces xinghaiensis* OF1 strain. World J. Microbiol. Biotechnol. 34, 1–13.

Yen, G.C., Duh, P.D., 1993. Antioxidant properties of methanolic extracts from peanut hull. J. Am. Oil Chem. Soc. 70, 383–386.